Nanotechnology **19** (2008) 175102 (6pp) doi:10.1088/0957-4484/19/17/175102

Quantum dot conjugated hydroxylapatite nanoparticles for *in vivo* imaging

Yan Guo[1], Donglu Shi[1], Jie Lian[2,3], Zhongyun Dong[4], Wei Wang[1], Hoonsung Cho[1], Guokui Liu[5], Lumin Wang[2] and Rodney C Ewing[2]

[1] Department of Chemical and Materials Engineering, University of Cincinnati, Cincinnati, OH 45221, USA
[2] Departments of Geological Sciences and Materials Science and Engineering, University of Michigan, Ann Arbor, MI 48109, USA
[3] Department of Mechanical, Aerospace and Nuclear Engineering, Rensselaer Polytechnic Institute, Troy, New York 12180, USA
[4] Department of Internal Medicine, University of Cincinnati, Cincinnati, OH 45221, USA
[5] Chemistry Division, Argonne National Laboratory, Argonne, IL 60439, USA

E-mail: shid@email.uc.edu

Received 18 July 2007, in final form 11 February 2008
Published 25 March 2008
Online at stacks.iop.org/Nano/19/175102

Abstract
Hydroxylapatite (HA) nanoparticles were conjugated with quantum dots (QDs) for *in vivo* imaging. The surface structures of HA nanoparticles with conjugated quantum dots (HA-QD) were studied by transmission electron microscopy (TEM) and laser fluorescent spectroscopy. The TEM data showed that the quantum dots were well conjugated on the HA nanoparticle surfaces. The laser fluorescent spectroscopy results indicated that the HA-QD exhibited promising luminescent emission *in vitro*. The initial *in vivo* experiments revealed clear images of HA-QD from the hypodermic injected area at the emission of 600 nm. Furthermore, the optimized *in vivo* images of HA-QD with near-infrared emission at 800 nm were visualized after intravenous injection. These luminescent HA-QD nanoparticles may find important applications as biodegradable substrates for biomarkers and in drug delivery.

1. Introduction

In the research of biomedical diagnosis using nanoparticles, one of the key challenges has been the design and development of a nanosurface structure with multiple functionalities. Due to complexity in the biological system, the nanostructures are often required to have several key features with high tunability and controllability of the surface properties. First, the surface of the nanoparticles must be treated with specific functional groups for the attachment of biological molecules. Second, for diagnosis, strong luminescence from the nanoparticle is expected in the desired visible range for *in vivo* imaging. Third, certain geometrical dimensions of the nanoparticle would be preferred for the storage and release of the treatment drugs. Finally, the nanoparticles or the substrate materials should be highly biodegradable in order to reduce the toxicity. So far, few attempts have been made in the design and development of a unique nanostructure that can meet all the requirements described above. Most nanospecies developed previously have caused considerable concerns due to their known or unknown health risks [1–3]. While extensive research on the biocompatibility and toxicity of nanomaterials has been carried out, it is highly desirable to search for nontoxic and biocompatible substrates for biomarking and drug delivery applications [3, 4]. Another important issue relates to the emission intensity of the luminescent nanoparticles. Although several types of nanoparticles have been found to exhibit visible and infrared emissions, their intensities are often too low for *in vivo* imaging [5–8]. For instance, single wall carbon nanotubes have been known to have emissions in the infrared range, but their weak intensity makes it not possible for deep tissue and whole-body *in vivo* imaging [5, 8].

Fluorescent proteins and small organic dyes have been used as fluorescent contrast agents for living animal imaging [9]. The ideal fluorescent probe would contain a fluorescent agent that emits light on target emission. Among all fluorescent nanomaterials, quantum dots have superior properties, including higher quantum yield and much sharper

emission spectra. Due to these unique properties, extensive research has been carried out on cancer diagnosis by using quantum dots [10–15]. Quantum dots have already shown promise as biosensors and live cell labels. Most of the previous studies on quantum dots were only based on cell-bioconjugated or polymer-encapsulated imaging experiments [15]. The oxidation of the quantum dot surfaces results in the release of divalent cadmium, known for its high toxicity. In extreme conditions, the acute cytotoxicity of cadmium was observed, and the slower release of quantum dots may result in chronic effects of cadmium [16]. Recently, Derfus *et al* used cultured liver cells to determine the cytotoxicity of CdSe/ZnS quantum dots with various surface coatings [17]. The results suggested that the surface coatings must be sufficiently stable to prevent the exposure and oxidation of cadmium. In this study, an alternative approach was used to prevent the release of divalent cadmium from quantum dots by using hydroxylapatite (HA) as a biocompatible substrate. HA nanoparticles were surface conjugated with quantum dots, leading to strong visible luminescence.

HA has been found to reduce the nonspecific deposition of quantum dots *in vivo* and is essentially nontoxic to cells and animals [18, 19]. In our previous research, it was demonstrated that it was possible to use HA for biomedical applications [20]. Furthermore, the surfaces of HA are quite porous, making it ideal for drug storage and delivery [21, 22]. In this present study, we report the experimental results of transmission electron microscopy (TEM) on the surface structures of HA nanoparticles conjugated with quantum dots (HA-QD). The optical behaviors of the functionalized HA-QD were studied by laser fluorescence spectroscopy. Initial *in vivo* imaging results are also presented, which were obtained from HA-QD hypodermic and intravenous injections.

2. Experimental details

2.1. Materials

The HA nanoparticles were synthesized using a microwave-assisted combustion with the auto-ignition–molten salt hybrid route [23]. Aqueous solutions containing $NaNO_3$, $Ca(NO_3)_2 4H_2O$, and KH_2PO_4 were irradiated in a microwave for 5 min at 600 W of power. The as-synthesized precursors were then stirred in water at room temperature for 1 h to obtain the HA nanoparticles. The synthesized HA powder has a size distribution of 50–100 nm [23].

The EviTags 600 quantum dots were purchased from Evident Technologies, NY. The quantum dot is consisted of a CdSe core and a shell of ZnS with polyethylene glycol (PEG) ligand surface coating. The inert PEG coating is stable *in vivo*. This coating stability is particularly suitable for rendering quantum dots biocompatible by changing the surface chemistry [24, 25], and for protecting the CdS/ZnS particles from oxidative reactions [17]. The PEG coating also allows greater vascular circulation time, but nonspecific uptake cannot be eliminated completely [25]. The quantum dots have the emission wavelength of 600 nm (QD_{600}) and hydrodynamic diameters of ∼20 nm. The CdSe/ZnS quantum dots were dispersed in water with the concentration of 12 nmol ml^{-1}. The Qdot 800 ITK quantum dots with emission wavelength of 800 nm (QD_{800}) were purchased from Invitrogen Corporation, CA. QD_{800} has a core of CdSeTe and a shell of ZnS with a surface coating of PEG. The CdSeTe/ZnS quantum dot was commercially packed in borate with the concentration of 8 nmol ml^{-1}.

2.2. Surface functionalization

The HA nanoparticles were sonicated for 2 h using a Fisher Scientific 100 sonic dismembrator. The well-dispersed HA nanoparticles were suspended in phosphate buffered saline (PBS) suspension with a concentration of 60 μmol ml^{-1}. To obtain quantum dots that can bind to the carboxyl functionalized HA nanoparticles, the quantum dots were functionalized with ethylenediamine in PBS for 8 h, which resulted in the amine functional group on their surfaces. In this procedure, the quantum dots, functionalized with amine terminal groups (QD-NH_2), were able to conjugate with HA [$Ca_5(PO_4)_3OH$] by the covalent reaction between amine and hydroxyl.

2.3. Fabrication of HA-QD conjugation

HA-QD conjugates were obtained using 1-(3-dimethylamino-propyl)-3-ethylcarbodiimide hydrochloride (EDC) in the presence of *N*-hydroxysuccinimide (NHS) [26]. In this experiment, NHS-activated HA intermediates were reacted with amine-activated quantum dots using EDC to produce HA-QD conjugation. The procedure for coupling the amine functionalized quantum dots to HA is illustrated in figure 1.

The reaction was completed in PBS at pH 7.4. The HA-QD suspension was incubated at 50 °C for 12 h. It was then cooled to room temperature, centrifuged for 30 min, and rinsed three times with PBS using centrifugation and decantation. The coupled HA-QD suspension was filtered through a 3.0 μm Teflon membrane and re-suspended in PBS. The concentration of conjugated quantum dots is 66.4 ppb (μg l^{-1}) for 1 μg HA nanoparticles in 1 ml of the PBS suspension.

2.4. Characterization of HA-QD conjugation

The surface morphology and microstructure of the HA-QD were studied using a JEOL 2010 F analytic transmission electron microscope. The samples were prepared by dispersing HA-QD suspensions directly on holey carbon films supported with Cu grids. Luminescent spectroscopy was performed to study the emissions of HA-QD and pure quantum dots. The luminescent spectra of HA-QD and pure quantum dots were obtained with Nd:YAG laser excitation of 355 nm and LED excitation of 475 nm, respectively. Fluorescent microscopy (Olympus 1X51) was performed to study the HA-QD under 350 nm of excitation without background light.

2.5. In vivo imaging of HA-QD conjugation

80 μl of HA-QD suspensions were injected into live nude mice. There were 66.4 ppb quantum dots in 1 μg HA per 1 ml of the PBS. The *in vivo* imaging of the mice was studied by using the Kodak Whole-Mouse Image Station (Kodak 4000MM). The excitation light from a high-intensity lamp with a 10×

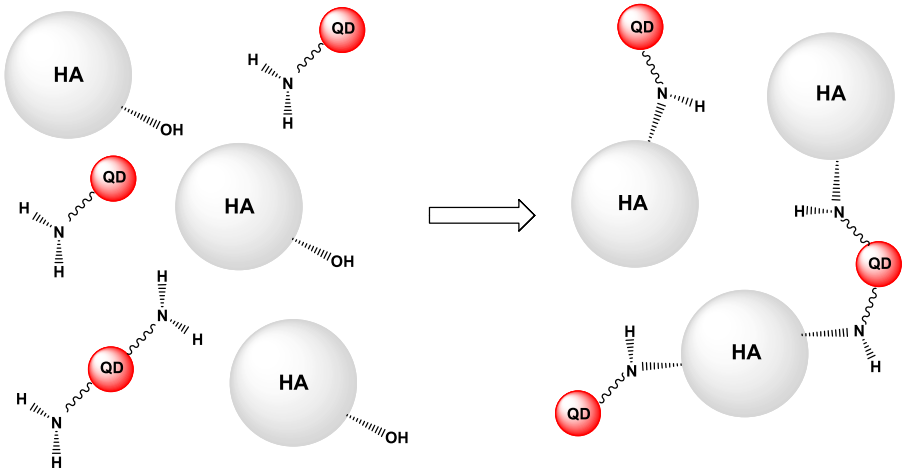

Figure 1. Schematic diagram showing the procedure for coupling the HA with amine-activated quantum dots. (This figure is in colour only in the electronic version)

zoom lens was directed through the selected excitation filter to the mice. Excitations of 465 and 720 nm were employed for emissions at 600 and at 800 nm, respectively.

The mice used for *in vivo* imaging were maintained in a facility approved by the American Association for Accreditation of Laboratory Animal Care and in accordance with current regulations and standards of the US Department of Agriculture, US Department of Health and Human Services, and National Institute of Health. This study was approved by Institutional Animal Use and Care Committee (IACUC) at the University of Cincinnati, OH.

3. Results and discussion

The low-magnitude TEM image of HA-QD (figure 2(a)) shows a typical morphology of HA nanoparticles with CdSe/ZnS quantum dots absorbed on their surfaces. From the Z-contrast image of the HA-QD (shown in figure 2(b)), we found that quantum dots can be easily differentiated from the substrate HA nanoparticles. The quantum dots have a quite uniform size distribution in the range between 5 and 10 nm and are randomly coupled on the HA nanoparticles whose dimensions (∼50 nm) are considerably larger than those of the quantum dots. High-resolution TEM images (figures 2(c) and (d)) clearly show the lattice structures of the CdSe/ZnS quantum dots and HA nanoparticles. These images indicate successful coupling of quantum dots onto the surfaces of HA nanoparticles. In figure 2(c), smaller quantum dots can be seen surrounding the HA particles while figure 2(d) shows a high density of quantum dots on the surface of a single HA particle. To further identify the conjugation of quantum dots on HA nanoparticle surfaces, an energy dispersive x-ray (EDX) spectrum was acquired (see figure 3). It shows the elemental signals from the CdSe/ZnS quantum dots, which is consistent with the TEM observations.

Figure 4 shows the normalized luminescence spectra observed from the pure quantum dots (dash dot line) and quantum dot conjugated HA (solid line). The luminescence spectrum of HA-QD is centered at 608 nm, an 8 nm red shift from the pure quantum dots whose peak intensity occurs at 600 nm. This demonstrates that the frequency of the photoluminescence in HA-QD is lower than that of pure quantum dots. However, in comparison to organic dyes such as rhodamine [27], the HA-QD system displays an emission spectrum that is nearly symmetric and much narrower in peak width, which is ideal for medical imaging diagnosis.

The fluorescent microscopy image of the HA-QD_{600} solution is shown in figure 5. It can be clearly seen that HA particles are spread across the dark background, exhibiting strong luminescence due to surface-coupled quantum dots. Note that some of the relatively larger luminescent spots result from the HA-QD conjugations as the individual nanoparticles may not be easily observed at this magnification. The PEG-grafted surface modification will be an affective way to eliminate the aggregation of nanoparticles [28]. This issue is being currently addressed in our research.

The images from deep tissues were obtained by intramuscularly injecting the HA-QD with the emission of 600 nm (HA-QD_{600}) into the rear leg muscles of the mice. Figure 6(a) shows the image of the control mouse, where only a background is observed. The injected locations in the deep tissues, as shown in figure 6(b), exhibit intense fluorescent signals from the HA-QD_{600}. This result clearly indicates that HA-QD can serve as an ideal biomarker candidate for *in vivo* imaging. However, emissions in this visible range below 700 nm can easily overlap with autofluorescences from the animal bodies as a background noise, such as the autofluorescence signals from skin wrinkles in the upper body (figure 6(b)). To further enhance the imaging contrast, particularly for deep tissue imaging, quantum dots with much longer emission wavelength of 800 nm were used to conjugate on HA nanoparticles (HA-QD_{800}). With the same procedure as that described above, HA-QD_{800} was intravenously (IV) injected into the tail veins of mice.

Figures 6(c) and (d) show the imaging results obtained from HA-QD_{800} immediately after IV injection into the tail veins of mice. As a result of high quantum yield and high absorbency, the fluorescence of HA-QD_{800} in the superficial vasculature (the whole tail vein in figure 6(c)) is readily visible

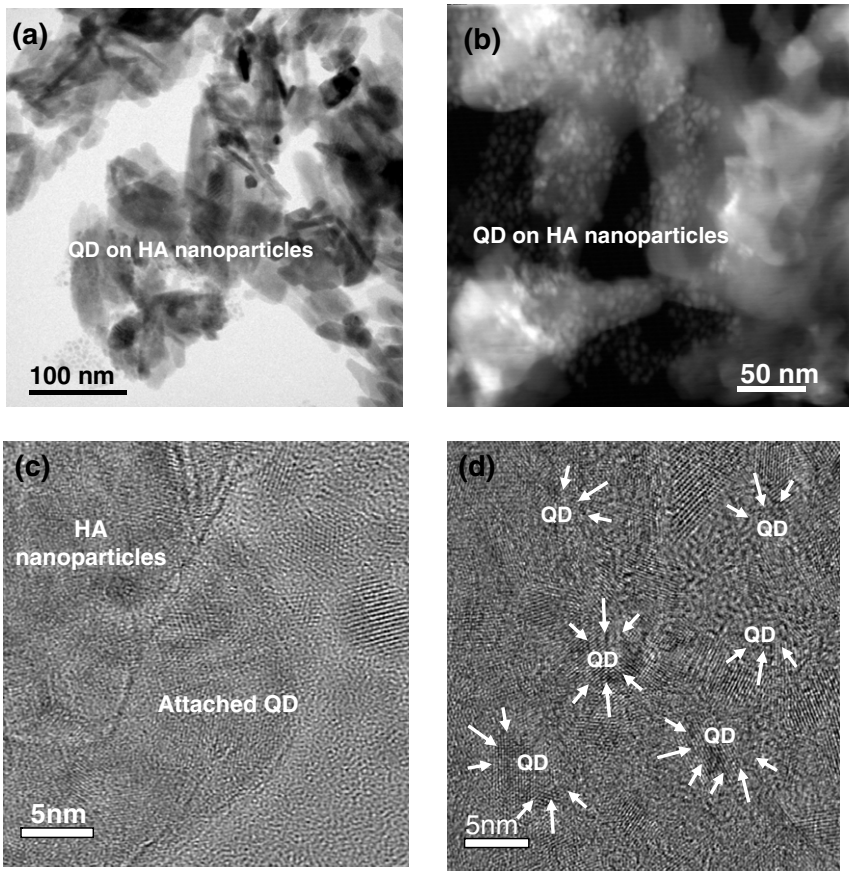

Figure 2. (a) A bright field TEM image of HA-QD showing a typical morphology of HA nanoparticle clusters with quantum dots; (b) a Z-contrast image showing quantum dots attached on the HA nanoparticle surface; (c) high-resolution TEM (HRTEM) image showing the lattice image of an HA nanoparticle and a quantum dot coupled together, and (d) HRTEM image of quantum dots on the top surface of a relatively large HA nanoparticle.

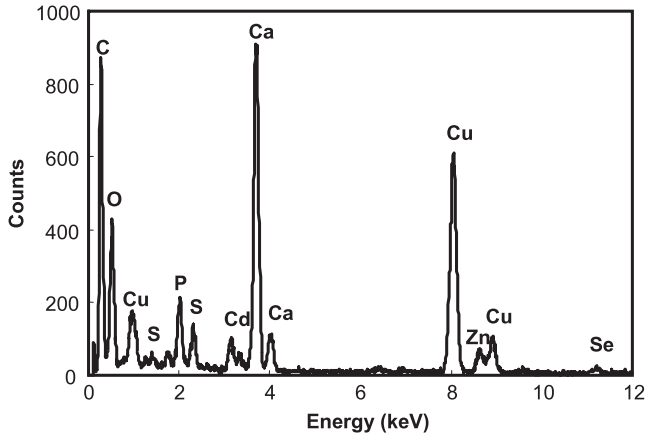

Figure 3. Energy dispersive x-ray (EDX) spectrum acquired from quantum dots attached on the surface of the HA nanoparticles. It shows the elemental signals from the CdSe/ZnS quantum dots and HA nanoparticles.

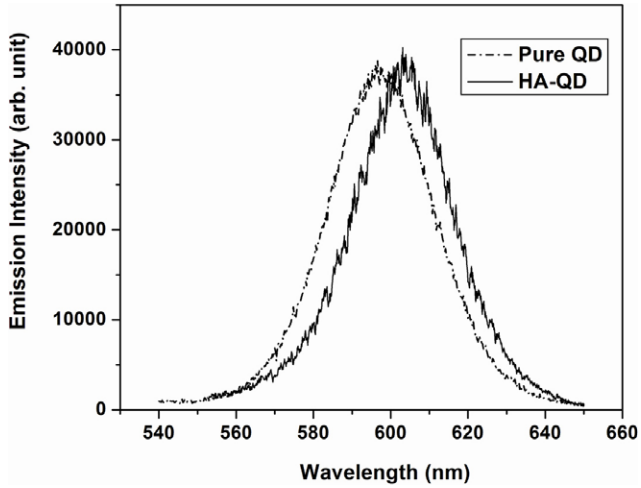

Figure 4. The luminescence spectra of pure EviTags 600 quantum dots (dash dot line) and HA-QD (solid line). The spectra were normalized to show the peak of pure quantum dots at 600 nm, and the peak of HA-QD at 608 nm, which has an 8 nm red shift from that for the pure quantum dots.

right after injection. However, at this early post-injection time, HA-QD_{800} cannot be imaged in organs, although the stomach has a little noise signal from the food autofluorescence. Upon migrating for 24 h, the image (figure 6(d)) shows the strong signals of HA-QD_{800} in both liver and spleen. The intense contrast image of inner organs with low-noise mouse background demonstrates the successful IV injection and circulation of HA-QD_{800} *in vivo*. The accumulation of HA-

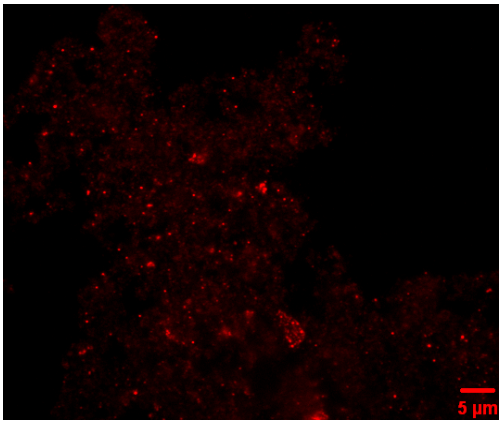

Figure 5. Fluorescent microscopy image (under 350 nm excitation) showing strong emissions from HA-QD_{600} against the dark background.

QD_{800} in the liver and spleen is due to the nanoparticles being easily uptaken by the reticuloendothelial system (RES, most notably in the liver) [29]. The efficient circulation and delivery of HA-QD_{800} in the live animal shows the high potential of HA-QD_{800} as a biomarker.

One of the challenges in biomedical diagnosis is deep tissue imaging by luminescent nanoparticles. As pointed out above, although some of the nanomaterials exhibit visible emissions, a few could result in clear and sharp images under the condition of deep tissue *in vivo* whole-body imaging. In this experiment, initial *in vivo* imaging was attempted in mice by IV injecting the HA-QD nanoparticles for the first time. In our previous research we have succeeded in synthesizing nanoparticles with surface-coated luminescent rare-earth materials [30, 31]. In this present study, the possibility of the conjugation of quantum dots onto nanoparticles was explored due to their superior optical properties. In a previous work, we also used carbon nanotubes as a substrate [32]. In the present study, we replaced carbon nanotubes with HA for its known biocompatibility and biodegradability. Furthermore, the surfaces of the HA nanoparticles are highly porous, making them ideal for storage and controlled release of drugs. This work is part of the design concept that we have employed on various nanoscale substrates. We believe that this concept can be extended into other biodegradable substrates.

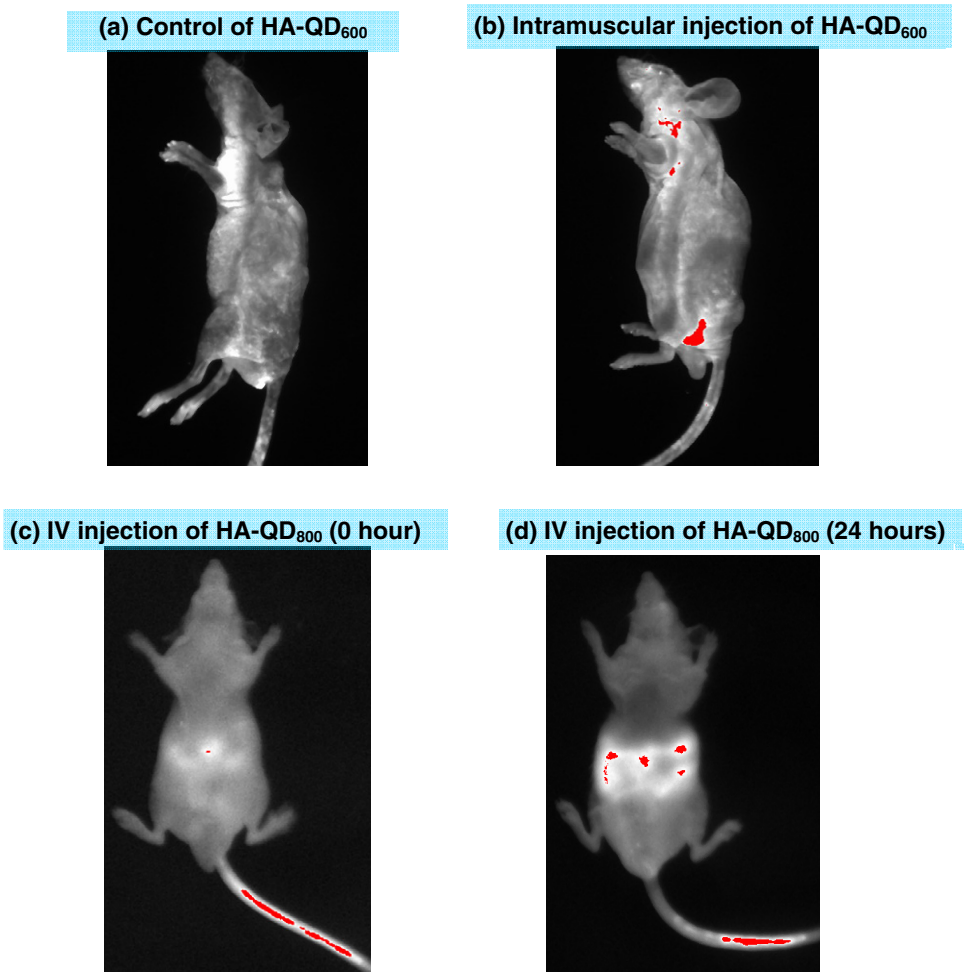

Figure 6. *In vivo* fluorescence images of (a) the control mouse before injection (only background autofluorescence); (b) HA-QD_{600} intramuscularly injected into the leg muscle (deep tissue) under 465 nm excitation; (c) HA-QD_{800} initially IV injected into the tail veins under 720 nm excitation, and (d) HA-QD_{800} IV post-injection, after circulation for 24 h.

4. Conclusion

In summary, quantum dots have been successfully coupled onto the surfaces of HA nanoparticles. The HA-QD interface coupling has been confirmed by TEM and EDX. The HA-QD suspensions have shown intensive fluorescence under various excitations. The HA-QD nanoparticles (both HA-QD_{600} and HA-QD_{800}) exhibit strong luminescent emissions in non-invasive optical *in vivo* imaging. The image contrast has been significantly enhanced by employing quantum dots with much longer emission at near-infrared, 800 nm. These results suggest a high possibility for HA-QD to be used as an effective biomarker in biomedical diagnosis. The development of HA-QD as a non-invasive optical *in vivo* imaging agent may have a great impact on the early detection, diagnosis, and treatment of cancer.

Acknowledgments

The work at University of Cincinnati (UC) was supported by a grant from UC Institute for Nanoscale Science and Technology. The work at Argonne National Laboratory was performed under the auspices of the Office of Basic Energy Science, Division of Chemical Sciences, US Department of Energy, under Contract No. W-31-109-ENG-38. The HA nanoparticles were provided by Dr Sarit B Bhaduri at the Department of Material Science and Engineering and Dr Xuejun Wen at the Department of Bioengineering at Clemson University.

References

[1] Hoet P H M, Nemmar A and Nemery B 2004 *Nat. Biotechnol.* **22** 19
[2] Colvin V L 2003 *Nat. Biotechnol.* **21** 1166
[3] Hoet P H M, Brüske-Hohlfeld I and Salata O 2004 *J. Nanobiotechnol.* **2** 3
[4] Krisanapiboon A, Buranapanitkit B and Oungbho K 2006 *J. Orthop. Surg.* **14** 315
[5] Cherukuri P, Gannon C J, Leeuw T K, Schmidt H K, Smalley R E, Curley S A and Weisman R B 2006 *Proc. Natl Acad. Sci.* **103** 18882
[6] Hai H, Guo Q X, Wee S C, Leong M G and Chwee H C 2002 *Nanotechnology* **13** 318
[7] Chen X Y, Yang L, Cook R E, Skanthakumar S, Shi D and Liu G K 2003 *Nanotechnology* **14** 670
[8] Liu Z, Cai W, He L, Nakayama N, Chen K, Sun X, Chen X and Dai H 2006 *Nat. Nanotechnol.* **10** 1038
[9] Bremer C and Weissleder R 2001 *Acad. Radiol.* **8** 15
[10] Jaiswal J K, Mattoussi H, Mauro J M and Simon S M 2003 *Nat. Biotechnol.* **21** 47
[11] Moghimi S M, Hunter A C and Murray J C 2001 *Pharmacol. Rev.* **53** 283
[12] Park S, Taton T A and Mirkin C A 2002 *Science* **295** 1503
[13] Gavin C *et al* 2002 *Nature* **415** 141
[14] Walt R 2005 *Science* **308** 217
[15] Gao X, Cui Y, Levenson R M, Chung L W K and Nie S 2004 *Nat. Biotechnol.* **22** 969
[16] Rikans L E and Yamano T 2000 *J. Biochem. Mol. Toxicol.* **14** 110
[17] Derfus A M, Chan W C W and Bhatia S N 2004 *Nano Lett.* **4** 11
[18] Rauschmann M A, Wichelhaus T A, Stirnal V, Dingeldein E, Zichner L, Schnettler R and Alt V 2005 *Biomaterials* **26** 2677
[19] Bishop A, Balázsi C, Yang J H C and Gouma P I 2006 *Polym. Adv. Technol.* **17** 902
[20] Wang W, Shi D, Lian J, Guo Y, Liu G K, Wang L M and Ewing R C 2006 *Appl. Phys. Lett.* **89** 183106
[21] Shi D, Jiang G and Wen X J 2000 *Appl. Biomater.* **53** 457
[22] Jarcho M 1981 *Clin. Orthop. Relat. Res.* **157** 2592
[23] Kutty M G, Loertscher J, Bhaduri S, Bhaduri S B and Tinga W R 2001 *Ceram. Eng. Sci. Proc.* **22** 3
[24] Wu X Y, Liu H J, Liu J Q, Haley K N, Treadway J A, Larson J P, Ge N F, Peale F and Bruchez M P 2003 *Nat. Biotechnol.* **21** 41
[25] Pellegrino T, Manna L and Kudera S 2004 *Nano Lett.* **4** 703
[26] Hermanson G T 1996 *Bioconjugate Techniques* (London: Academic) pp 8–9
[27] Chan W C, Maxwell D J, Gao X, Bailey R E, Han M and Nie S 2002 *Curr. Opin. Biotechnol.* **13** 40
[28] Baraton M I 2003 *Synthesis, Functionalization and Surface Treatment of Nanoparticles* (Gref. Ruxandra: American Scientific Publishers) chapter 11
[29] Akerman M E, Chan W C W, Laakkonen P, Bhatia S N and Ruoslahti E 2002 *Proc. Natl Acad. Sci.* **99** 12617
[30] Chen X Y, Yang L, Cook R E, Skanthakumar S, Shi D and Liu G K 2003 *Nanotechnology* **14** 670
[31] Lian J, Yang L, Chen X Y, Liu G K, Wang L M, Ewing R C and Shi D 2006 *Nanotechnology* **17** 1351
[32] Shi D, Guo Y, Dong Z Y, Lian J, Wang W, Liu G K, Wang L and Ewing R 2007 *Adv. Mater.* **19** 4033